J|A|C|S ARTICLES

Published on Web 08/28/2009

Understanding the Torquoselectivity in 8π-Electrocyclic Cascade Reactions: Synthesis of Fenestradienes versus Cyclooctatrienes

Catherine Hulot,[§] Shadi Amiri,[‡] Gaëlle Blond,[§] Peter R. Schreiner,*[,‡] and Jean Suffert*[,§]

Faculté de Pharmacie, Université de Strasbourg (UMR 7200 CNRS/UDS), 74 Route du Rhin, 67401 Illkirch/Strasbourg, France, and Institut für Organische Chemie, Justus-Liebig-Universität Giessen, Heinrich-Buff-Ring 58, D-35392 Giessen, Germany

Received May 19, 2009; E-mail: jean.suffert@pharma.u-strasbg.fr; prs@org.chemie.uni-giessen.de

Abstract: Unusual and novel polycyclic cyclooctatrienes, fenestradienes, and fenestrenes form readily from trienynes depending on the structure of the starting trienynes and the reaction conditions. The experimentally observed high torquoselectivities and complete diastereoselectivities of the 8π-electrocyclization products have been thoroughly studied using density functional computations at B3PW91/6-31G(d,p). The different *P*- and *M*-helical topologies for the Möbius aromatic transition structures are the origin of the observed torquoselectivities in the cyclooctatrienes. The *P*-helical topologies direct the newly formed single bonds into a favorable *equatorial* position of the neighboring cycloalkane moieties (**X** = ring size) that retain their most stable conformation. The *M*-helical transition structures lead to an *axial* connection for the smaller rings (**X** = 4−6) and an *equatorial* connection for the seven- and eight-membered cycloalkanes. This leads to unfavorable conformations for the larger cycloalkane moieties. Experiments and computations show that for trienynes involving small neighboring cycloalkane groups (**X** = 4−6) *M*-helical topology is preferred toward cyclooctatrienes and in the following the corresponding fenestradienes can be formed as kinetic or even thermodynamic products; they convert to their more stable cyclooctatriene valence isomers derived from *P*-helical transition structures at higher temperatures. For larger cycloalkane moieties with more conformational flexibility only cyclooctatrienes with torquoselectivities derived from *P*-helical transition structures form.

1. Introduction

Electronic as well as steric effects determine the sense of rotation of the substituents at terminal double bonds (inward or outward) in electrocyclic reactions. This *torquoselectivity* concept was first developed for the 4π-conrotatory cycloreversions of cyclobutene ring-openings,[1,2] and it has been extended to other types of reactions, such as 8π-conrotatory electrocyclizations.[3] Utilizing *ab initio* molecular orbital theory, Houk and co-workers demonstrated that, in contrast to 4π-conrotatory ring-openings of 3-substituted cyclobutenes, which are dominated by electronic effects of the substituents, steric effects determine the torquoselectivities of the 8π-conrotatory electrocyclizations of 1-substituted 1,3,5,7-octatetraenes.[3] Indeed, transition structures with substituents in the outward positions are preferred irrespective of the electronic nature of the substituents. Recently, Cossio et al. used density functional theory (DFT) to confirm these findings and the Möbius aromatic nature of a helical transition structure,[4] as previously reported by Houk et al.[5]

Scheme 1. Conversion of 1,3,5,7-Tetraenes to Bicyclo[4.2.0]octadienes

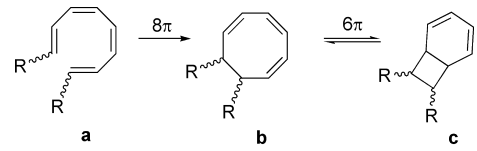

In most cases, the 8π-electrocyclization of 1,3*Z*,5*Z*,7-octatetraenes to cyclooctatrienes is followed by a 6π-electrocyclization to give bicyclo[4.2.0]octadienes (Scheme 1). Therefore, there are only few examples of stable cyclooctatrienes (**b**) in the literature. Indeed, in 1967 Kröner reported the spontaneous interconversion of **a** directly to **c**.[6] In contrast to his proposed mechanism, Huisgen and co-workers proposed cyclooctatriene intermediates (**b**), and that these electrocyclic reactions occur through spontaneous 8π-conrotatory and 6π-disrotatory electrocyclizations.[7] These contributions were the first experimental proofs of the Woodward−Hoffmann rules.

[§] Université de Strasbourg.
[‡] Justus-Liebig-Universität Giessen.

(1) Rondan, N. G.; Houk, K. N. *J. Am. Chem. Soc.* **1985**, *107*, 2099–2111.
(2) (a) Kallel, E. A.; Wang, Y.; Spellmeyer, D. C.; Houk, K. N. *J. Am. Chem. Soc.* **1990**, *112*, 6759–6763. (b) Rudolf, K.; Spellmeyer, D. C.; Houk, K. N. *J. Org. Chem.* **1987**, *52*, 3708–3710. (c) Spellmeyer, D. C.; Houk, K. N. *J. Am. Chem. Soc.* **1988**, *110*, 3412–3416.
(3) Thomas, B. E.; Evanseck, J. D.; Houk, K. N. *J. Am. Chem. Soc.* **1993**, *115*, 4165–4169.
(4) Lecea, B.; Arrieta, A.; Cossio, F. P. *J. Org. Chem.* **2005**, *70*, 1035–1041.
(5) Thomas, B. E.; Evanseck, J. D.; Houk, K. N. *Isr. J. Chem.* **1993**, *33*, 287–293.
(6) Kröner, M. *Chem. Ber.* **1967**, *100*, 3172–3182.
(7) Huisgen, R.; Dahmen, A.; Huber, H. *J. Am. Chem. Soc.* **1967**, *89*, 7130–7131.

 © 2009 American Chemical Society

Scheme 2. 7-Methylcycloocta-1,3,5-triene: An Example for an Isolated Natural Cyclooctatriene[14]

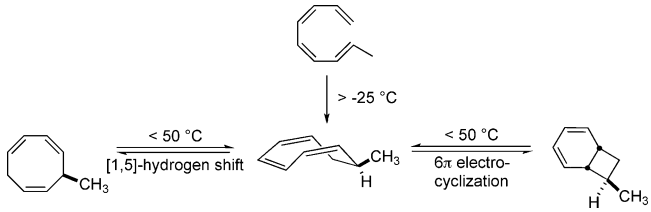

Such $8\pi-6\pi$-electrocyclization cascades were elegantly used for the total synthesis of several natural products.[8] A similar $8\pi-6\pi$-cascade strategy was used for the syntheses of elysiapyrones A and B,[9] coprinolone,[10] vitamin A,[11] functionalized bicyclo[4.2.0]octadienes,[12] and bicyclo[4.2.0]octenones.[13] Owing to the fast conversion of **b** to **c**, there are almost no natural products containing a cyclooctatriene system. To the best of our knowledge, 7-methylcycloocta-1,3,5-triene is the only example that could be isolated by Boland from the marine brown algae *Cutleria multifida* in trace amounts (Scheme 2).[14] This compound is stable at temperatures below 50 °C, but cyclizes or undergoes a [1,5]-hydrogen shift at higher temperature. Similarly, only a few groups have reported the synthesis of stable cyclooctatrienes. For example, Okamura synthesized an analogue of 9α,19-methano-1α,25-dihydroxyvitamin D_3 containing a cyclooctatriene system by mild hydrogenation of a trienyne followed by an 8π-electrocyclization.[15] Flynn and Ma reported the synthesis of various stable cyclooctatrienes by subsequent [1,5]- or [1,7]-hydrogen migration followed by 8π electrocyclization.[16] Only few other examples of isolated cyclooctatrienes were described.[17]

We previously reported a new method for the synthesis of tetracyclic cyclooctatrienes **13** and **14** (Scheme 3, path I).[18] These polycyclic molecules include eight-membered ring moieties, which are present in many biologically active natural products.[19] The key step for the preparation of these compounds is a one-pot cascade reaction discovered in our laboratory,[20] starting from a 4-*exo*-dig cyclocarbopalladation of the five- and six-membered ring propargylic diols **1** and **2**, followed by Stille coupling with tributylstannyldienes **6**, leading to the tetraenes **7** and **8**. These tetraenes spontaneously undergo an 8π-conrotatory electrocyclization to yield **13** and **14**. A large number of valuable polycyclic cyclooctanoids were prepared using this strategy from a variety of propargylic diols and tributylstannyldienes.[21] Although the yields were moderate, they are partly compensated by the complexity of these highly functionalized molecules.

To improve the efficiency of this process and to alter the functionalities in the molecules, we decided to use a new strategy (Scheme 3, path II). In this new approach, six- and seven-membered ring trienynes **4** and **5** were synthesized from diols **2** and **3** in a sequence of six reaction steps with good overall yields. Our results on the semihydrogenation of trienynes **4** at room temperature were recently reported (Scheme 3, path IIa):[22] the expected cyclooctatrienes **15** and/or **16** were not observed. Actually, we realized an unexpected $8\pi-6\pi$-cyclization cascade that ultimately led to the formation of [4.6.4.6]fenestradienes **21** and [4.6.4.6]fenestrenes **25**. These compounds were obtained in one-pot operation after a remarkable cascade of reactions.

En Route to the Fenestranes. The fascinating structures of the fenestranes, defined as doubly α,α′-bridged spiroalkanes, have been examined extensively for more than 35 years, particularly from theoretical viewpoints.[23] These studies focused mainly on exploring the degree of planarity around the central carbon atom, as well as their stability, strain, and reactivity. The planarization around the central carbon is due to minimizing strain of the all-spiro fused rings.[23a] These constraints make the syntheses of fenestranes challenging.

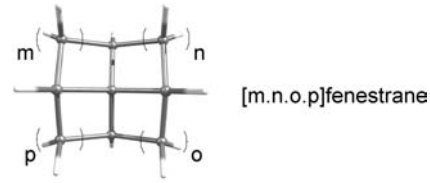

Several new syntheses of fenestranes have recently been achieved, improving access to these compounds by shortening the

(8) Beaudry, C. M.; Malerich, J. P.; Trauner, D. *Chem. Rev.* **2005**, *105*, 4757–4778.
(9) (a) Barbarow, J. E.; Miller, A. K.; Trauner, D. *Org. Lett.* **2005**, *7*, 2901–2903. (b) Cueto, M.; D'Croz, L.; Mate, J. L.; San-Martin, A.; Darias, J. *Org. Lett.* **2005**, *7*, 415–418. (c) Parker, K. A.; Wang, Z. *Org. Lett.* **2006**, *8*, 3553–3556.
(10) Lawrence, A. L.; Wegner, H. A.; Jacobsen, M. F.; Adlington, R. M.; Baldwin, J. E. *Tetrahedron Lett.* **2006**, *47*, 8717–8720.
(11) Vogt, P.; Schlageter, M.; Widmer, E. *Tetrahedron Lett.* **1991**, *32*, 4115–4116.
(12) Pineschi, M.; Del Moro, F.; Crotti, P.; Macchia, F. *Eur. J. Org. Chem.* **2004**, *2004*, 4614–4620.
(13) Snider, B. B.; Harvey, T. C. *J. Org. Chem.* **1994**, *59*, 504–506.
(14) (a) Pohnert, G.; Boland, W. *Tetrahedron* **1994**, *50*, 10235–10244. (b) Pohnert, G.; Boland, W. *Nat. Prod. Reports* **2002**, *19*, 108–122.
(15) Hayashi, R.; Fernandez, S.; Okamura, W. H. *Org. Lett.* **2002**, *4*, 851–854.
(16) (a) Kerr, D. J.; Willis, A. C.; Flynn, B. L. *Org. Lett.* **2004**, *6*, 457–460. (b) Ma, S.; Gu, Z. *J. Am. Chem. Soc.* **2006**, *128*, 4942–4943. (c) Zhu, Y.; Guo, Y.; Zhang, L.; Xie, D. *J. Comput. Chem.* **2007**, *28*, 2164–2169.
(17) (a) Brückner, S.; Baldwin, J. E.; Adlington, R. M.; Claridge, T. D. W.; Odell, B. *Tetrahedron* **2004**, *60*, 2785–2788. (b) Dell'Erba, C.; Mugnoli, A.; Novi, M.; Pertici, M.; Petrillo, G.; Tavani, C. *Eur. J. Org. Chem.* **1999**, 431–435. (c) Magomedov, N. A.; Ruggiero, P. L.; Tang, Y. *J. Am. Chem. Soc.* **2004**, *126*, 1624–1625.
(18) Salem, B.; Suffert, J. *Angew. Chem., Int. Ed.* **2004**, *43*, 2826–2830.
(19) (a) Mehta, G.; Singh, V. *Chem. Rev.* **1999**, *99*, 881–930. (b) Petasis, N. A.; Patane, M. A. *Tetrahedron* **1992**, *48*, 5757–5821.
(20) (a) Bour, C.; Blond, G.; Salem, B.; Suffert, J. *Tetrahedron* **2006**, *62*, 10567–10581. (b) Salem, B.; Klotz, P.; Suffert, J. *Org. Lett.* **2003**, *5*, 845–848. (c) Salem, B.; Klotz, P.; Suffert, J. *Synthesis* **2004**, 298–307. (d) Suffert, J.; Salem, B.; Klotz, P. *J. Am. Chem. Soc.* **2001**, *123*, 12107–12108.
(21) Lautens, M.; Smith, N. D.; Ostrovsky, D. *J. Org. Chem.* **1997**, *62*, 8970–8971.
(22) Hulot, C.; Blond, G.; Suffert, J. *J. Am. Chem. Soc.* **2008**, *130*, 5046–5047.
(23) (a) Coates, R. M.; Muskopf, J. W.; Senter, P. A. *J. Org. Chem.* **1985**, *50*, 3541–3557. (b) Rowley, M.; Kishi, Y. *Tetrahedron Lett.* **1988**, *29*, 4909–4912. (c) Paquette, L. A.; Liang, S.; Galatsis, P. *Synlett* **1990**, 663. (d) Snider, B. M.; Yang, K. *J. Org. Chem.* **1992**, *57*, 3615–3626. (e) Wender, P. A.; Nuss, J. M.; Smith, D. B.; Suarez-Sobrino, A.; Vagberg, J.; Decosta, D.; Bordner, J. *J. Org. Chem.* **1997**, *62*, 4908–4909. (f) Lo, P. C.-K.; Snapper, M. L. *Org. Lett.* **2001**, *3*, 2819–2821. (g) Ruprah, P. K.; Cros, J.-P.; Pease, J. E.; Whittingham, W. G.; Williams, J. M. J. *Eur. J. Org. Chem.* **2002**, *314*, 5–3152. For excellent reviews in this field see: (h) Keese, R. *Chem. Rev.* **2006**, *106*, 4787–4808. (i) Mehta, G.; Srikrishna, A. *Chem. Rev.* **1997**, *97*, 671–720. (j) Venepalli, B. R.; Agosta, W. C. *Chem. Rev.* **1987**, *87*, 399–410. (k) Tellenbroker, J.; Kuck, D. *Eur. J. Org. Chem.* **2001**, 1483–1489. (l) Bredenkotter, B.; Barth, D.; Kuck, D. *Chem. Commun.* **1999**, 847–848. (m) Kuck, D. *Liebigs Ann.-Recl.* **1997**, 1043–1057. (n) Kuck, D.; Schuster, A.; Gestmann, D.; Posteher, F.; Pritzkow, H. *Chem. Eur. J.* **1996**, *2*, 58–67.
(24) Gerber, P.; Keese, R. *Tetrahedron Lett.* **1992**, *33*, 3987.
(25) (a) Wender, P. A. M.; Dore, T.; deLong, M. A. *Tetrahedron Lett.* **1996**, *37*, 7687. (b) Wender, P. A.; deLong, M. A.; Wireko, F. C. *Acta Crystallogr.* **1997**, *C53*, 954. (c) Chappell, D.; Russell, A. T. *Org. Biomol. Chem.* **2006**, 4409–4430. (d) Cornelisse, J. *Chem. Rev.* **1993**, *93*, 615–669. (e) McCullough, J. J. *Chem. Rev.* **1987**, *87*, 811–860.

Scheme 3. Differences in the Reactivities of Tetraenes **7**−**12** Giving Cyclooctatrienes **13**−**18**, Fenestradienes **19**−**24**, and [4.6.4.6]Fenestradienes **25**[a]

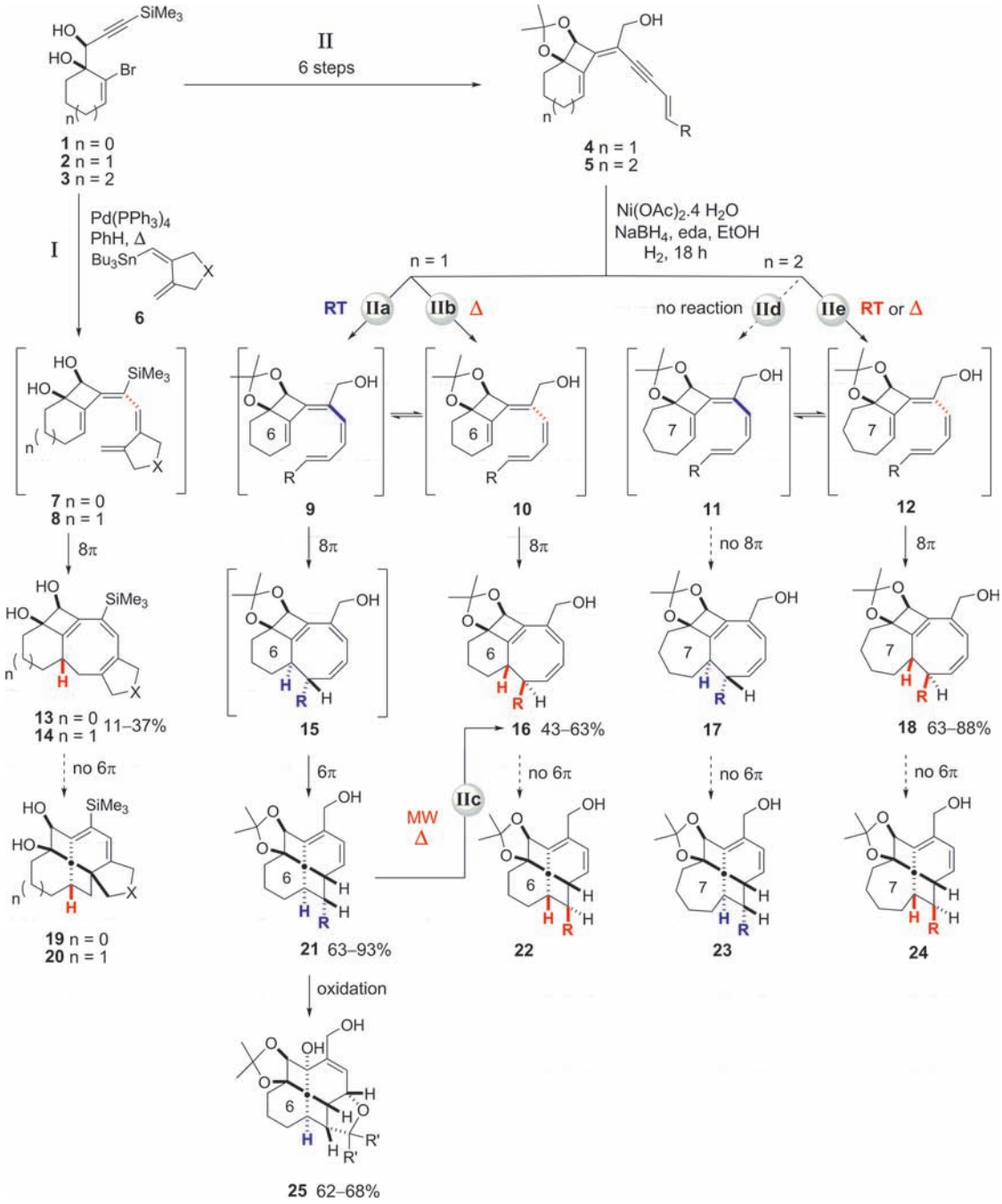

[a] The bold or dashed single CC bonds in **7**−**12** refer to the orientation of the open chain relative to the dioxolane. For the case R = $C(CH_3)_2OH$ in the path II, the nomenclature of the compound includes an "**a**" after the numbering such as **21a** (for computations, vide infra). Similar to the allenes, we use a bold dot for the carbon in the middle of the fenestrane structure to avoid confusion. Eda = ethylenediamine.

number of steps and increasing the yields when compared to early approaches in this field.[24] Intramolecular arene-olefin photocycloadditions,[25] photoinduced [2 + 2] cycloadditions,[26] transition metal-induced cyclizations,[27] and cascade reactions[28] are current state-of-the-art methods to prepare this class of compounds.

Here, we describe a detailed account and extensions of this original strategy to the rapid and efficient syntheses of this class of structurally complex compounds **21** and **25**. We disclose our findings on the different reactivities of starting compounds **4** and **5** upon semihydrogenation.

This paper includes computations that aid in the understanding of the underlying mechanistic questions, that is, the torquoselectivity in electrocyclization reactions. We rationalize the stereochemical issues during the 8π-conrotatory electrocyclizations of tetraenes **7**−**12**. Moreover, these computations provide a basis for understanding the divergence in reactivities of compounds **13**, **14**, **16**−**18** on the one hand and **15** on the other.

2. Results and Discussion

Preparation of Trienynes 4 and 5. In this approach, six- and seven-membered ring trienynes **4** and **5** were synthesized from diols **2** and **3** in a sequence of six reactions in good overall yields (Scheme 4). The preparation of trienynes **4**

Scheme 4. Synthesis of Trienynes **4** and **5**

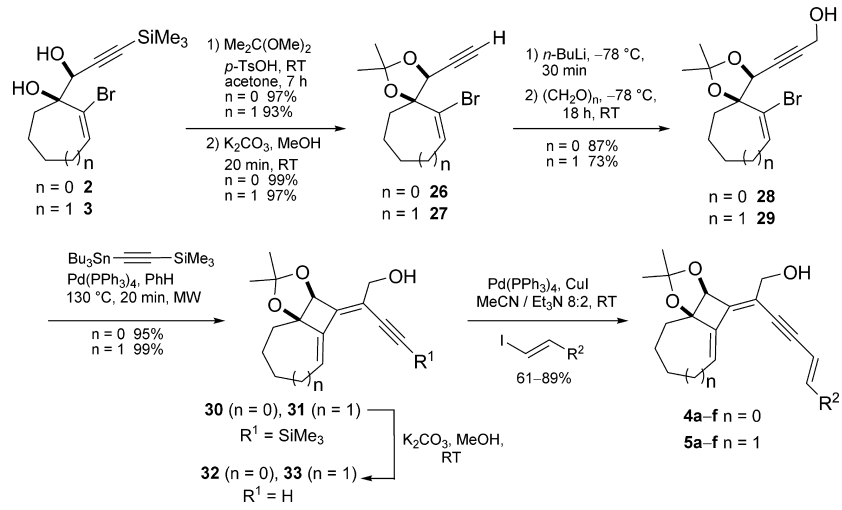

Table 1. Optimization of the Selective Partial Hydrogenation of Trienyne **4a**

entry	catalyst	equiv. cat.	solvent	H_2 [atm]	yield **21a** [%][a] (**4a**)
1	Lindlar[b]	0.1	AcOEt/EtOH	1	0 (100)
2	Lindlar[c,e]	0.1	MeOH	5	20 (0)
3	Zn(0)/CuBr[d]		EtOH/THF	1	0 (70)
4	$NiCl_2/NaBH_4$[b]	0.2	EtOH	1	0 (100)
5	$Ni(OAc)_2 \cdot 4\ H_2O$/BER[c]	0.1	MeOH	1	0 (100)
6	$Ni(Acac)_2/NaBH_4$[b]	0.2	EtOH	1	26 (74)
7	$Ni(Acac)_2/NaBH_4$[c,e]	0.2	EtOH	1	40 (60)
8	$Ni(Acac)_2/NaBH_4$[c,e]	0.2	EtOH	5	35 (65)
9	$Ni(Acac)_2/NaBH_4$[c,e]	0.2	EtOH	5	0 (100)
10	P-2 Ni[b]	0.2	EtOH	1	0 (100)
11	P-2 Ni[c]	0.2	EtOH	1	92 (8)
12	P-2 Ni[c]	0.2	EtOH	1	36 (64)
13	P-2 Ni[c,f]	0.2	EtOH	1	60 (40)
14	P-2 Ni[c,e]	0.2	EtOH	1	93[g] (7)
15	P-2 Ni[c,e]	0.2	EtOH	1	15 (85)
16	**P-2 Ni**[c,e]	**1**	**EtOH**	**1**	**88 (0)**

[a] Determined by ^1H NMR of the crude product. [b] Trienyne **4a** prepared by a modified Sonogashira protocol. [c] Trienyne **4a** prepared by classical Sonogashira coupling. [d] Excess (40 equiv) of Zn metal. [e] Trienyne **4a** treated with ethanolamine before hydrogenation. [f] Trienyne **4a** treated with EDTA-Na_2 before hydrogenation. [g] Yield of 62% after chromatography on silica gel.

was described in our preceding paper.[22] Starting diol **3** was prepared by addition of a suitably protected metalated propargylic alcohol to bromocycloheptenone, followed by deprotection and chromatographic separation of the *anti* and *syn* diastereomers.[20d] After protection of the diol function of **3** with 2,2-methoxypropane and removal of the trimethylsilyl group, the free alkyne **27** was metalated with *n*-butyllithium in THF at −78 °C, followed by addition of paraformaldehyde. Propargylic alcohol **29** was isolated in good overall yield (66%) over three steps. The key 4-*exo*-dig cyclocarbopalladation/Stille cross coupling was conducted on **29** as described previously,[22] in the presence of [Pd-$(PPh_3)_4$] (10 mol %) as catalyst under microwave irradiation in benzene at 130 °C. These conditions afforded cleanly the bicyclic [5.2.0] product **31** in 99% yield after 20 min of irradiation. Removal of the trimethylsilyl group under basic conditions was conducted without isolation of the terminal alkyne **33** due to its propensity to polymerize. Alkyne **33** was immediately submitted to Sonogashira cross coupling, with [$Pd(PPh_3)_4$], CuI and several vinyl iodides to give compounds **5a**−**f** in 79−86% yields in two steps (see Supporting Information).

Optimization of the Reaction Conditions for the Monohydrogenation of Trienynes. With the key substrates in hand, efforts turned toward effecting the selective hydrogenation of the conjugated alkyne function. The optimization of the reaction conditions was carried out using the six-membered ring trienyne **4a** (Scheme 3, path IIa, R = $C(CH_3)_2OH$). Several catalysts, well-known for their ability to partially hydrogenate a triple bond, were selected and tested. Unexpectedly, in most cases it turned out that only traces of [4.6.4.6]fenestradiene **21a** were isolated after these monohydrogenation assays.

As summarized in Table 1, the use of Lindlar catalyst/H_2 in AcOEt/EtOH (entry 1)[29] or in MeOH at RT[30] under 5 atm of H_2 pressure was not successful, only leading to the new cyclized product **21a** in small amounts (20%) and several unidentified side products (entry 2). Reaction of trienyne **4a** with the Zn/Cu couple[31] at 80 °C in EtOH/THF gave some decomposition with unchanged starting material (entry 3). Several nickel boride (Ni_2B) catalysts were prepared from a Ni^{II} source and $NaBH_4$, and tested. $NiCl_2/NaBH_4$[32] and a supported nickel boride catalyst prepared from $Ni(OAc)_2 \cdot 4\ H_2O$ and a borohydride exchange

(26) (a) Crimmins, M. T. *Chem. Rev.* **1988**, *88*, 1453–1473. (b) De Keukeleire, D.; He, S. L. *Chem. Rev.* **1993**, *93*, 359–380. (c) Crimmins, M. T.; Mascarella, S. W.; Bredon, L. D. *Tetrahedron Lett.* **1985**, *26*, 997–1000. (d) Keese, R. *Angew. Chem. Int. Ed.* **1992**, *31*, 344–345.
(27) (a) de Meijere, A. *Chem. Rev.* **2000**, *100* (8), 2739–3282. (b) Kulinkovich, O. G.; de Meijere, A. *Chem. Rev.* **2000**, *100*, 2789. (c) Yet, L. *Chem. Rev.* **2000**, *100*, 2963. (d) Tsuji, J. *Transition Metal Reagents and Catalysts*; Wiley & Sons: Sussex, 2000; (e) Beller, M., Bolm, C., Eds. *Transition Metals for Organic Synthesis*; Wiley-VCH: Weinheim, 1998. (f) Nakamura, I.; Yamamoto, Y. *Chem. Rev.* **2004**, *104*, 2127. (g) Zeni, G.; Larock, R. C. *Chem. Rev.* **2004**, *104*, 2285. (h) Hartwig, J. F. In *Comprehensive Coordination Chemistry II*; Cleverty, Mc- J. A., Meyer, T. J., Eds.; Elsevier: Oxford, U.K., 2004; Vol. 9, p 369.
(28) (a) Kim, D. H.; Son, S. U.; Chung, Y. K.; Lee, S.-G. *Chem. Commun.* **2002**, 56. (b) Son, U. K.; Park, K. K. H.; Chung, Y. K. *J. Am. Chem. Soc.* **2002**, *124*, 6838.
(29) Lindlar, H. *Helv. Chim. Acta* **1952**, *35*, 446–450.
(30) (a) Aerssens, M. H. P. J.; Brandsma, L. *J. Chem. Soc., Chem. Commun.* **1984**, 735–736. (b) Aerssens, M. H.; Heiden, P. J.; van der, R.; Heus, M.; Brandsma, L. *Synth. Commun.* **1990**, *20*, 3421–3425.
(31) (a) Brown, C. A. *J. Org. Chem.* **1970**, *35*, 1900–1904. (b) Brown, C. A.; Ahuja, V. K. *J. Org. Chem.* **1973**, *38*, 2226–2230.
(32) Choi, J.; Yoon, N. M. *Tetrahedron Lett.* **1996**, *37*, 1057–1060.
(33) Brown, C. A.; Ahuja, V. K. *J. Chem. Soc., Chem. Commun.* **1973**, 553–554.

Scheme 5. Synthesis of the Cyclooctatriene **16a**

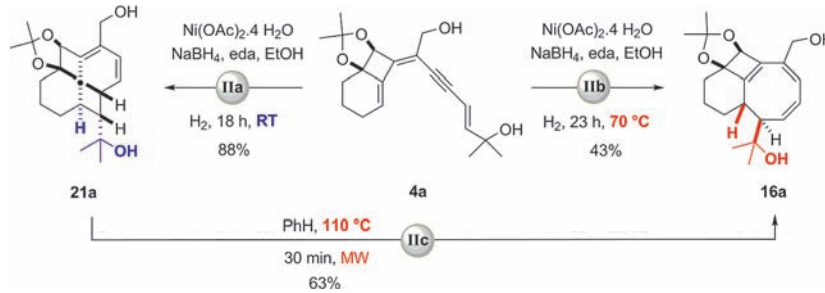

Table 2. Synthesis of Fenestradienes and Fenestrenes

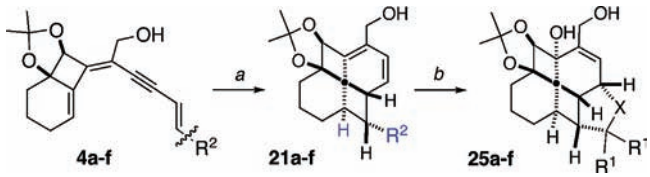

Entry	Starting compd.	R^2	Product	Yield [%][c]	Product	X	Yield [%][d]
1	**4a**	$C(CH_3)_2OH$	**21a**	88	**25a** R^1 = Me	O	63, (57)[e]
2	**4b**	CH_2OH	**21b**	[f]	**25b** R^1 = H	O	35[g]
3	**4c**	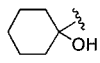	**21c**	86	**25c** $R^1 = (CH_2)_5$	O	68
4	**4d**		**21d**	93	**25d** $R^1 = (CH_2)_4$	O	62
5	**4e**		**21e**	63[h]	**25e** R^1 = *i*Bu	O	67
6	**4f**	$(CH_2)_5CH_3$	**21f**	90	–	–	–

[a] P-2 Ni, 1 equiv., EDA, EtOH, H_2, 1 atm. [b] *m*-CPBA, $NaHCO_3$, CH_2Cl_2, 0 °C, 20 min to 1 h. [c] Yield determined by ^{1}H NMR of the crude. [d] Yield of isolated product after chromatography. [e] Neat, under air/O_2. [f] Not determined. [g] Yield for the two steps (a,b) from **4b**. [h] The product **21e** was contaminated by 30% of inseparable **4e**.

Table 3. Synthesis of 7-4-8 Fused Polycycles **18**

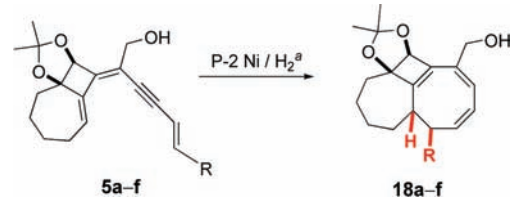

Entry	Trienyne	R	Product	Yield [%][b]
1	**5a**	$C(CH_3)_2OH$	**18a**	77
2	**5b**	$(CH_2)_5CH_3$	**18b**	63
3	**5c**		**18c**	81
4	**5d**		**18d**	81
5	**5e**	CH_2CH_2Ph	**18e**	76
6	**5f**	$C(iBu)_2OH$	**18f**	88

[a] P-2 Ni, 1 equiv., eda, EtOH, H_2, 1 atm. [b] Yield of isolated product after chromatography.

resine (BER): $Ni(OAc)_2 \cdot 4\ H_2O$/BER,[33] showed no reactivity allowing for the full recovery of trienyne **4a** (entries 4 and 5). $Ni(Acac)_2$ was chosen as an alternative for the generation of Ni(0). Disappointingly, the cyclized product **21a** was only obtained in low yield when the reaction was conducted under 1 atm of H_2 (26−40%, entries 6 and 7) and failed under 5 atm (entries 8 and 9). Several analogous experiments using 20% of P-2 Ni, a nickel boride catalyst prepared from $Ni(OAc)_2 \cdot 4\ H_2O$/$NaBH_4$, in ethanol at room temperature in the presence of ethylenediamine (EDA) and hydrogen (1 atm) were engaged.[34]

In those experiments trienyne **4a** was prepared through classical Sonogashira coupling (5% $Pd(PPh_3)_4$, CuI 15%, Et_3N, MeCN). The cascade reaction was always capricious, but in several cases afforded cyclized materials **21a** in 36−93% yields (entries 11−15). When trienyne **4a** was prepared through a modified Sonogashira protocol starting from the silylated alkyne (1.2 equiv of ICH = $CHC(Me)_2OH$, MeCN/Et_3N 8:2, RT, 13 h, 2 equiv of CuCl),[28] the partial hydrogenation was totally ineffective (entry 10). These studies indicated eventually that residual copper salts would interfere with the Ni-catalyzed reduction and subsequent electrocyclizations. To avoid the presence of copper salts, we decided to use the classical Sonogashira conditions with only 15% CuI. The crude trienyne **4a** was shaken vigorously with ethanolamine for 1 h to trap the copper through complexation. If a small amount of copper salt was present in the starting compound, the hydrogenation catalyst was rapidly inhibited as indicated by the solution color change from black to yellow. Moreover, because of the sensitivity of the P-2 Ni catalyst prepared from $Ni(OAc)_2 \cdot 4\ H_2O$, we decided to explore the influence of the amount of the P-2 Ni used for the partial hydrogenation of the triple bond. Gratifyingly, when 1 equivalent of P-2 Ni was used, the starting diol was almost totally consumed and resulted in the formation of the [4.6.4.6]fenestradiene **21a** in 88% reproducible yield as determined ^{1}H NMR spectroscopy (Table 1, entry 16).

This efficient cascade involves three consecutive transformations starting from trienynes **4**: an initial mild hydrogenation using a P-2 Nickel catalyst at room temperature, followed by 8π-conrotatory and 6π-disrotatory electrocyclizations. The obtained [4.6.4.6]fenestradienes **21** reacted with oxygen (air) in a final cyclization to give [4.6.4.6]fenestrenes **25** (Table 2).

Synthesis of New Cyclooctatrienes 16 and 18. Surprisingly, the semihydrogenation of six-membered ring trienynes **4** at 70

(34) Marshall, J. A.; Chobanian, H. R.; Yanik, M. M. *Org. Lett.* **2001**, *3*, 4107–4110.
(35) Frisch, M. J., et al. *Gaussian 03*, Revision C.02; Gaussian, Inc.: Wallingford, CT, 2004.
(36) (a) Schreiner, P. R. *Angew. Chem., Int. Ed.* **2007**, *46*, 4217–4219. (b) Schreiner, P. R.; Fokin, A. A.; Pascal, R. A.; de Meijere, A. *Org. Lett.* **2006**, *8*, 3635–3638. (c) Navarro-Vazquez, A.; Schreiner, P. R. *J. Am. Chem. Soc.* **2005**, *127*, 8150–8159.

Scheme 6. Reactivity of Trienyne **5d**

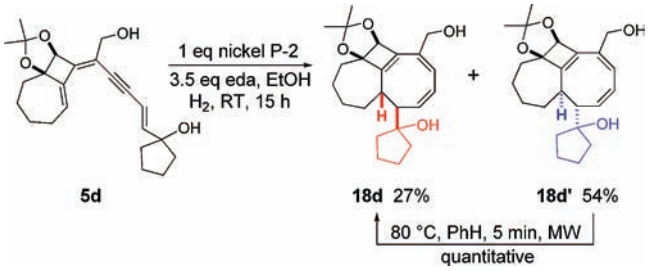

Scheme 7. Reactivity of the Seven-Membered Polycycle **18a**

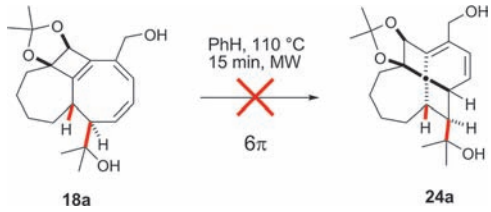

°C gave different results regarding the structure and the torquoselectivity. The only isolated product was the 6-4-8 fused system **16** (Schemes 3 and 5, path IIb). In this case, we did not obtain the [4.6.4.6]fenestradiene **21** formed when the reaction was carried out at room temperature (path IIa). It is important to note that the two tetraene conformers **9** and **10** gave the initial cyclooctatrienes **15** and **16** through an 8π-conrotatory electrocyclization process following *opposite* torquoselectivity (Scheme 3, paths IIa and IIb). Interestingly, the isolated [4.6.4.6]fenestradiene **21a** converted completely into the cyclooctatriene **16a**, after heating in benzene at 110 °C under microwave irradiation for 30 min (Schemes 3 and 5, path IIc). There was no degradation. This behavior was observed only for one example but identical results are expected on the other fenestradienes. This work is currently underway and will be reported in due course. The precedent results show a remarkable kinetic versus thermodynamic control in the respective formation of **21a** (kinetic control) and **16a** (thermodynamic control). The reason for the torquoselectivity observed in the preferential formation of product **21a** under kinetic control is not well understood and further experiments to probe this question are currently underway. The reversibility of this complex process (retro 6π electrocylization−retro 8π electrocylization−8π electrocyclization) and the complete control of the stereoselectivity of those reactions have not been reported previously in the literature.

As reported in the introduction (Scheme 3, paths IId and IIe), the same kind of stable cyclooctatriene **18** was obtained when the seven-membered ring trienynes **5** were hydrogenated under the optimized conditions. The only products isolated in 63 to 88% yields were the stable 7-4-8 fused systems **18** (Table 3). Reactions were again completely stereoselective in all cases except **5d**. Tetraene **12** produced the stable cyclooctatriene **18** with opposite torquoselectivity as compared to the formation of the intermediate cyclooctatriene **15** from tetraene **9** (Scheme 3, paths IIa and IIe), but with the same configuration as in the formation of the stable cyclooctatriene **16** from tetraene **10** (Scheme 3, paths IIb and IIe).

In only one case, (R = $(CH_2)_4COH$), two new cyclooctatrienes **18d** and **18d′** were isolated in a 27/54 ratio coming from an 8π-electrocyclization with the two possible torquoselectivities. The diastereoisomer **18d′** (kinetic product) slowly rearranged to give the other diastereomer **18d** (thermodynamic product) at room temperature. This process took only 5 min when the mixture of **18d** and **18d′** was heated under microwave irradiation at 80 °C in benzene (Scheme 6). Eventually, **18d** was isolated in 81% yield.

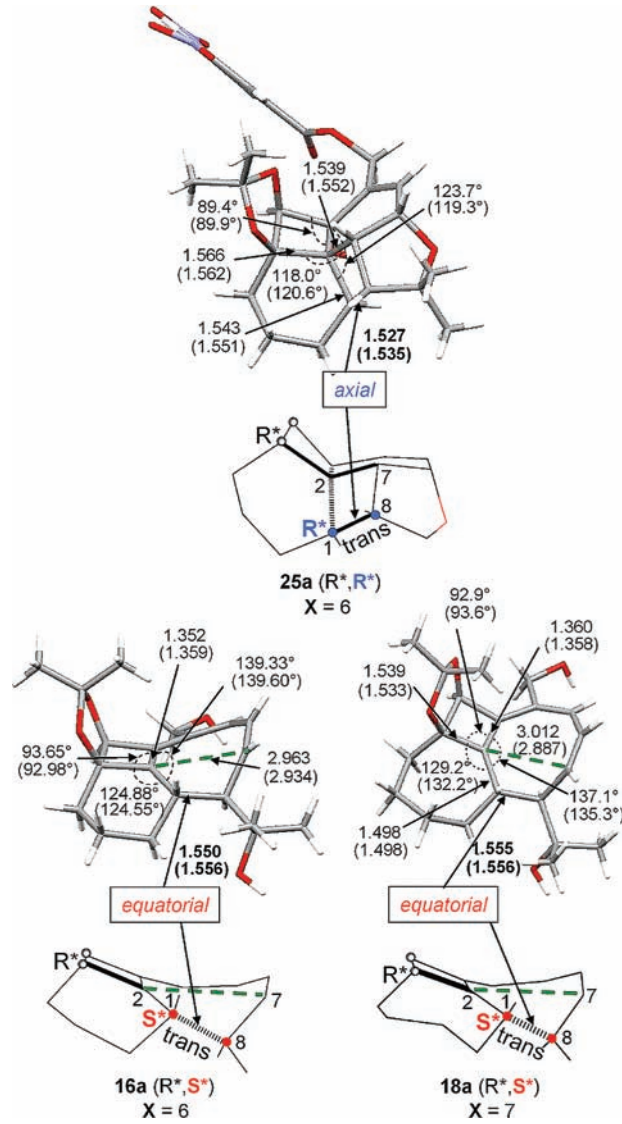

Figure 1. X-ray structural analyses of the nitrobenzoate derivate of fenestrene **25a**[22] and cyclooctatrienes **16a** and **18a**. Selected B3PW91/6-31G(d,p) computed parameters in parentheses; bond lengths in Å. The simplified X-ray structures beneath show the different diastereomeric products caused by opposite torquoselectivities to form new C^1-C^8 single bonds in the 8π-conrotatory ring closures. The relative configurations of the stereogenic centers are shown by (R*,**R***) and (R*,**S***) symbols.

In addition, heating of cyclooctatriene **18a** under microwave irradiation in benzene at 110 °C for 15 min gave no trace of [4.6.4.7]fenestradiene **24a** (Scheme 7).

The structures of all compounds were elucidated following extensive ^{13}C and 2D ^1H NMR, NOESY, COSY, HSQC, and HMBC experiments as well as mass spectral analysis. Eventually, new structures **16a** and **18a** were unambiguously confirmed by X-ray diffraction analysis (computational section, Figure 1). We previously reported the X-ray crystal structure of the nitrobenzoate derivative of the [4.6.4.6]fenestrene **25a**.[5]

3. DFT Computations

Models and Methods. This part of the study focuses on identifying the factors that determine the formation of fenes-

Scheme 8. Model Systems for the Computational Investigations

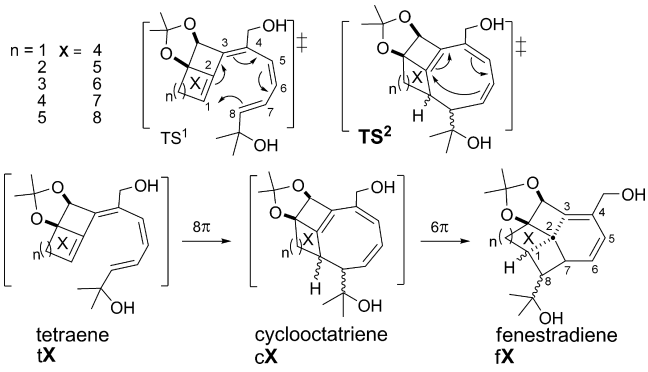

tradienes vs cyclooctatrienes in the cascade reactions. This includes the examination of the relevant stereochemistries. We focus on the influence of the size of the cyclic alkene moiety (**X**, Scheme 8) as the key variable that determines the strain during the cascade reactions. The nomenclature t**X**, c**X**, and f**X** refers to the tetraenes, cyclooctatrienes, and fenestradienes, respectively, including olefinic rings with size **X**. Scheme 8 presents the computational model compounds including starting tetraenes (t**X**) where **X** indicates four- to eight-membered rings. For the computations $-C(CH_3)_2OH$ was used for R-group.

We analyze the following: assessment of the aromaticities of the transition structures by using structural and magnetic criteria, frontier molecular orbital analyses of the torquoselectivities, conformational interconversions of the olefinic ring moieties, and potential energy hypersurfaces.

The Gaussian 03 suite[35] was used for all computations. We employed the hybrid functional B3PW91 with the standard Pople 6-31G(d,p) basis set and characterized all stationary points as minima (NIMAG = 0) or transition structures (NIMAG = 1). This level of theory reproduces the energy differences of hydrocarbons well, also when comparing isomers differing in the relative numbers of single and double bonds.[36] All geometries were fully optimized without symmetry constraints; zero-point vibrational energy (ZPVE) corrections were applied to the absolute energies.

The molecular orbitals are discussed on the basis of Kohn−Sham orbitals and also complete active space self-consistent field CASSCF(8,8) (based upon Hartree−Fock orbitals) computations on equilibrium DFT geometries. The CASSCF results are available in the Supporting Information and they agree quantitatively well with those at the Kohn−Sham level. NMR and nucleus-independent chemical shielding[37] NICS(0) computations in the geometric ring centers were done with GIAO[38]-B3LYP/6-311G(d,p)//B3PW91/6-31G(d,p) on the optimized geometries.

Structural Analyses of the Cyclooctatrienes and the [4.6.4.6]Fenestrenes. As the agreement between the experimental and computed structures is quite good (see for comparison **16a**, **18a**, and **25a** in Figure 1), we assume this will also apply to other related structures under consideration.

As noted in the experimental section all steps of the cascade reaction are stereospecific. Owing to the observed stereochemistry, 8π-conrotatory electrocyclizations from the tetraenes lead to *trans* connections in all cyclooctatrienes (Figure 1). We conclude that the active conformation leading to the transition structures must be *s-cis* at the two rotatable single bonds in the *exo*-triene chain. As a consequence, the R-group (for computations R = $-C(CH_3)_2OH$) is oriented *outward* before ring closure occurs (Figure 2). Recently, DFT studies by Cossio et al. suggested this outward orientation for such 8π-electrocyclic reactions, independent of the π-donor or π-acceptor character of the substituent;[4] this is in marked contrast to thermal 4π-electron conrotatory electrocyclizations.[1] This generalization was rationalized on the basis of secondary orbital interactions, electrostatics, and steric effects.[4]

Rotations of terminal substituents in the right- and left-handed directions (opposite torquoselectivities) during the 8π-conrotatory mode cause *trans* connections giving the observed *opposite* (R*,**R***)- and (R*,**S***)-stereochemistries in the cyclooctatrienes (Figure 2). Two different orientations of the triene open chain in the transition structures relative to the dioxolane moiety make the right- and left-handed rotations possible. When the open chain is oriented on the same side of the dioxolane (*M*-helical configuration), the right-handed rotation is possible for the terminal substituents and the (R*,**R***)-stereoisomer of c**X** results. However, in the (R*,**S***)-diastereomer the dioxolane and the open chain are placed on opposite sides (*P*-helical configuration) and the C^1-C^8 bond forms through a left-handed rotation. In the case of cyclooctatriene **15a** and in the following fenestrene **25a** the newly formed C^1-C^8 bond is oriented *axially* through a *M*-helical topology, while it adopts an *equatorial* configuration

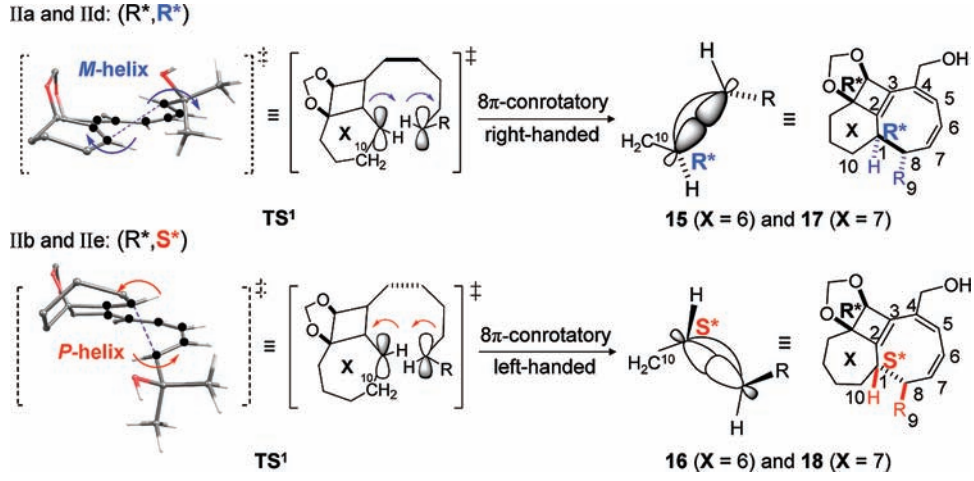

Figure 2. Opposite torquoselectivities in the 8π-conrotatory cyclizations leading to *trans* connections. B3PW91/6-31G(d,p) *M*- and *P*-helical Möbius aromatic transition structures for the first ring closure. Some of the atoms were omitted for clarity.

Table 4. B3PW91/6-31g(d,p) Geometric Analysis for TS[1] with Different Ring Sizes and B3LYP/6-31G(d,p)//B3PW91/6-31G(d,p) Total NICS(0) Values [ppm] in the Ring Centers of the Selected Eight-Membered Ring

X	$C^1-C^8_{termini}$	C^2-C^3	$r-^a$	$\Delta r_m{}^b$	$<C^1C^2C^3$ °	ϕ $C^{10}C^1C^8C^9$ °	NICS(0)[c]
4	2.191	1.386	1.399	0.010	150.1	+60.8	–11.2
5	2.258	1.395	1.397	0.009	149.8	+35.7	–10.6
6	2.245	1.402	1.398	0.007	140.2	+9.7	–11.1
7	2.223	1.406	1.400	0.006	133.0	–6.3	–10.9
8	2.220	1.404	1.401	0.003	131.4	–14.3	–10.1

[a] Mean bond length for the delocalized chain including C^1 to C^8 [Å]. [b] Maximum deviation from the mean bond length [Å]; per definition the amount smaller than 0.06 Å indicates an aromatic character. [c] NICS(0) for the benzene as the reference system at the same level of chemistry is −8.9 ppm.

Table 5. B3PW91/6-31G(d,p) Geometry Analyses for **TS[2]** toward (R*,**R***)-Fenestradiene

X	$C^2-C^7_{termini}$	C^2-C^3	$r-^a$	$\Delta r_m{}^b$	ϕ $C^3C^2C^7C^6$ °	ϕ $C^4C^5C^6C^7$ °	NICS(0)[c]	NICS(0)[d]
4	2.254	1.393	1.401	+0.009	7.3	–24.3	–10.7	–8.9
5	2.185	1.408	1.402	–0.012	6.9	–25.2	–11.1	–10.2
6	2.154	1.406	1.403	–0.015	16.9	–24.9	–12.3	–11.3
7	2.093	1.434	1.400	–0.010	5.8	–28.3	–11.6	–10.8
8	2.144	1.412	1.404	–0.014	16.7	–25.9	–12.3	–11.4

[a] Mean bond length for the delocalized chain including C^2 to C^7 [Å]. [b] Maximum deviation from the mean bond length [Å]. [c] Ghost atom was inserted into center of the selected six-membered ring including C^2 to C^7. [d] Ghost atom was inserted into center of the selected eight-membered ring including C^1 to C^8.

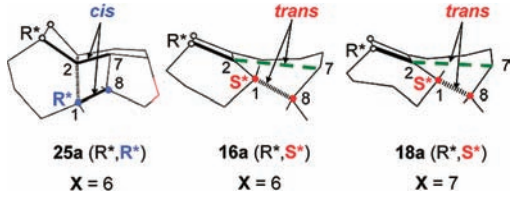

Figure 3. Simplified X-ray structures of the nitrobenzoate derivative of fenestrene **25a**[22] and cyclooctatrienes **16a** and **18a**. The C^1-C^8 and C^2-C^7 bonds in (R*,**R***)-fenestrene (**25a**) indicate a *cis*-orientation, but a *trans*-orientation in (R*,**S***)-stereoisomer extended from **16a** and **18a**.

in **16a** and **18a** by a *P*-helical configuration in the first transition structures (Figures 1 and 2).

The C^2-C^7 bonds converting the cyclooctatrienes to the fenestradiene valence isomers through the 6π-disrotatory electrocyclization step have a *fixed* orientation relative to the **X**-membered rings (bold in Figure 3). The C^1-C^8 bond that forms in the previous reaction step requires *the same* orientation relative to C^2-C^7 for formation of a fenestradiene isomer, that is, a *cis* orientation is required. This is given only by *M*-helical topology in the first transition structure (right-handed torquoselectivity) corresponding for the (R*,**R***)-stereochemistry. Hence, only (R*,**R***)-fenestrene **25a** can form from intermediate **15a** because this steric requirement is not given in the cyclooctatrienes **16a** and **18a** (Figure 3).

Aromaticities of the Helical Transition Structures. The first electrocyclization reaction from the 1*Z*,3*Z*,5*Z*,7*E*-octatetraenes (t**X**) occur through Möbius type aromatic transition structures to produce the corresponding cyclooctatrienes; *M*- and *P*-helical shapes of the open chain in the transition structures are presented in Figure 2. The formally antiaromatic (8π-electron) Hückel system would be particularly unfavorable. In 1964, Heilbronner predicted already that such 4n π-systems with a Möbius topology (C_2 symmetry) would be closed-shell aromatic molecules.[39] The first explicit example of such a system was suggested in 1998 for $C_9H_9^+$,[40] and in 2003 the first stable Möbius annulene crystal structure for an aromatic hydrocarbon was reported by Herges et al.[41] The deviation from C_2 symmetry in the Möbius moieties of the optimized transition structures for **X** = 6 and 7 is very small. The maximum deviations from the mean C−C bond lengths (Δr_m) and the negative NICS(0)

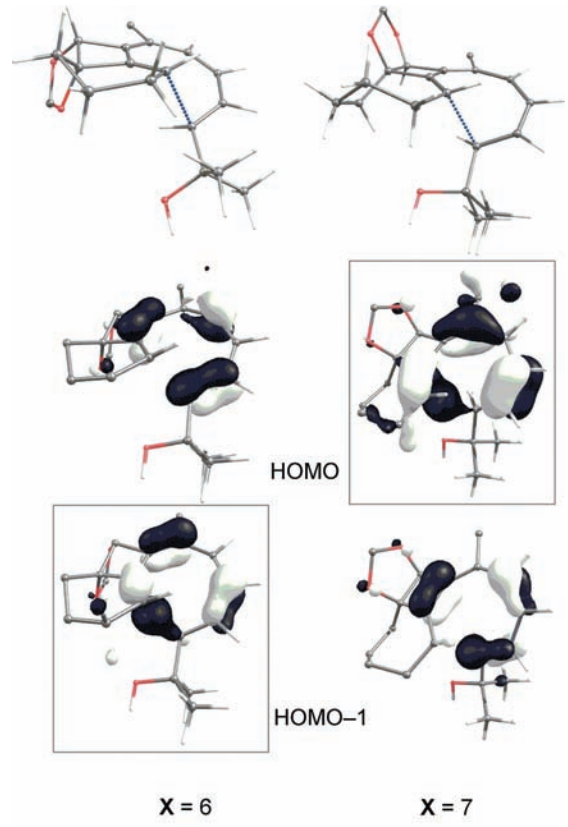

Figure 4. B3PW91/6-31G(d,p) Contour plots for the C^1-C^8 bonding molecular orbitals of two **TS[1]** **X** = 6 and 7 (R*,**R***- and R*,**S***-stereoisomers as examples, respectively). The HOMO-1 and HOMO for **X** = 6 and 7, respectively, show favorable overlap for the 8π-conrotatory process. The contour value was chosen ±0.05 au for the HOMO for **X** = 7 and for the other orbitals it is ±0.06 au. Some atoms have been omitted for clarity.

(37) Würthwein, E. U.; Chandrasekhar, J.; Jemmis, E. D.; Schleyer, P. v. R. *Tetrahedron lett.* **1981**, *22*, 843–846.
(38) Wolinski, K.; Hinton, J. F.; Pulay, P. *J. Am. Chem. Soc.* **1990**, *112*, 8251–8260.
(39) Heilbronner, E. *Tetrahedron Lett.* **1964**, *29*, 1923–1928.
(40) Mauksch, M.; Gogonea, V.; Jiao, H.; Schleyer, P. v. R. *Angew. Chem., Int. Ed.* **1998**, *37*, 2395–2397.

Figure 5. B3PW91/6-31G(d,p) Hückel aromatic topology for **TS²** leading to fenestradiene (here **X** = 6 as an example). The HOMO shows a 6π-electron disrotatory connection; contour value at ±0.06 au.

values indicate significant aromaticity for all transition structures for the first cyclization. Changes in the ring sizes (**X**) cause only little variation of the aromaticity indicators (Table 4).

The frontier molecular orbital analyses provide more information about the chemical bonding in the first transition structures. In 1964, Heilbronner determined that all electron levels for a Möbius type perimeter with 4n π-electrons will be degenerate.[39] The Möbius character of the cyclization transition structures is evident from the shapes and nodal planes in the occupied molecular orbitals (Figure 4). For **X** = 6 HOMO−1 shows the typical Möbius topology with three nodal planes; for **X** = 7 the HOMO display these aromatic bonding features.

Rearrangement of the 1,3,5-Cyclooctatriene Moiety (COT) to Valence Isomer Bicyclo[4.2.0]octa-2,4-diene (BCO). The second transition structure for the interconversion of COT→BCO gives fenestradiene through a 6π-electron disrotatory electrocyclic process. The C_8H_{10} valence isomers COT and BCO have received much attention since Cope et al. confirmed that the syntheses of COT derivatives typically lead to equilibrium mixtures of COT and BCO products.[42]

The molecular orbitals for the second transition structures show two nodal planes, which agree well with a low-energy aromatic Hückel system. The dihedral angles between the vicinal double bonds of the cyclohexadiene moieties are less than 30° (Table 5) so that the conjugation interaction of the π-bonds is still significant (Figure 5). The more negative NICS(0) values in the centers of the cyclohexadiene moieties of the transition structures as compared to the complete eight-membered ring moieties, indicate higher degree of aromaticity. These transition structures become increasingly unfavorable with increasing the size of the aliphatic ring (**X**).

Conformational Analyses of the Aliphatic Moieties. The crystal structures show the most stable chair and twist chair conformers for the six- and seven-membered rings of **16a** and **18a**, respectively (Figure 1). The six-membered ring of fenestradiene **21a** (the unoxidized precursor of **25a**) reveals a half chair (envelope) form, which is known to be a transition structure for interconversion of the chair and twist boat conformers of cyclohexane. *In that sense*, **21a** is one of the few isolable molecules that show this conformation. We

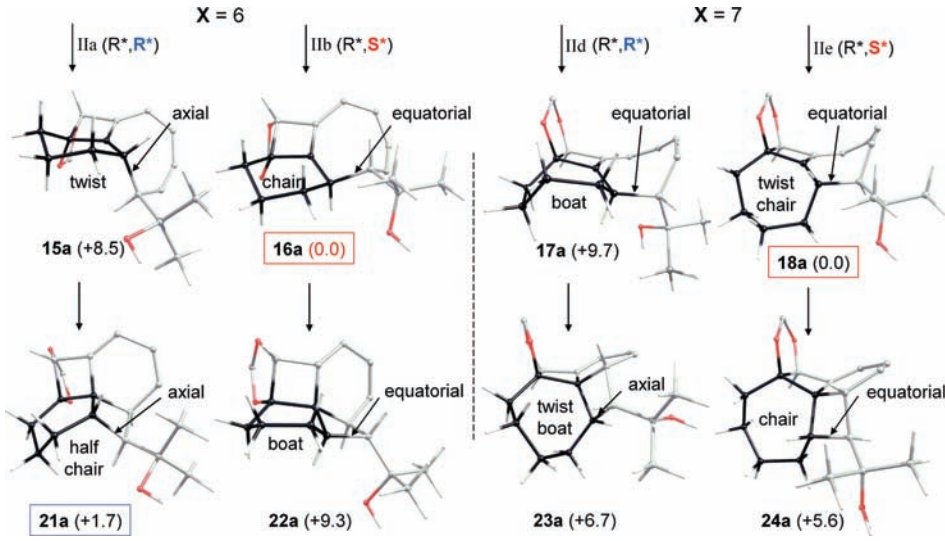

Figure 6. Conformational interconversions of the two six- and seven-membered ring moieties in cyclooctatrienes and fenestradienes. The experimentally observed structures are boxed.

Table 6. B3PW91/6-31G(d,p) Conformational Analyses for c**X** and f**X**, when **X** = 6 and 7

no. (**X**)	rel. config. of the new bond formed	conformation of cycloalkane	new bond(s) rel. to cycloalkane[a]	rel. config. of C^1-C^8 and C^2-C^7 in f**X**	ϕ $C^1C^8C^7C^2$ °	C^2-C^7 Å in f**X**	central angles ° in f**X**	relative energies in kcal mol^{-1}
15a (**6**)	(R*,**R***)	twist	ax	–	–	–	–	+8.5 (not obs.)
16a (**6**)	(R*,**S***)	chair	eq	–	–	–	–	0.0 (obs.)
17a (**7**)	(R*,**S***)	boat	eq	–	–	–	–	+9.7 (not obs.)
18a (**7**)	(R*,**S***)	twist chair	eq	–	–	–	–	0.0 (obs.)
21a (**6**)	(R*,**R***)	half chair	ax/ax	*cis*	15.0	1.554	127.0/121.8	+1.7 (obs.)
22a (**6**)	(R*,**S***)	boat	eq/eq	***trans***	**23.1**	1.590	142.8/123.0	+9.3 (not obs.)
23a (**7**)	(R*,**R***)	twist boat	ax/ax	*cis*	17.8	1.559	125.0/121.7	+6.7 (not obs.)
24a (**7**)	(R*,**S***)	chair	eq/eq	***trans***	**22.6**	1.586	136.5/123.2	+5.6 (not obs.)

[a] ax and eq indicate axial and equatorial positions, respectively.

Scheme 9. Potential Energy Hypersurfaces for the Two Stereochemical Controls in Pathway I[a]

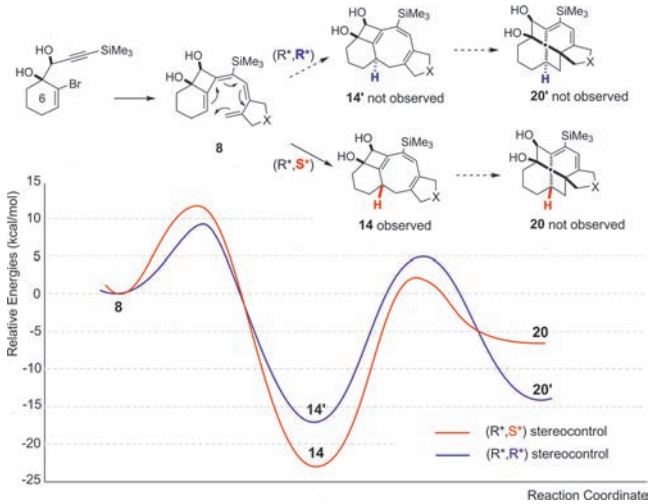

[a] X = $C(CO_2Me)_2$ for computations.

examined all possible conformations of the cycloalkane moieties of **15a**−**24a** and compared them with the three experimentally isolated compounds (Figure 6).

The 8π-conrotatory as well as the 6π-disrotatory cyclization determines the aliphatic ring moiety's relative configuration. It seems that in cyclooctatrienes with (R*,**S***)-configurations the cycloalkane moieties adopt their most stable conformers: chair (**16a**, Figure 6) and twist chair (**18a**). An axial orientation of the newly formed bond is unfavorable because it introduces additional strain in the aliphatic ring (**15a**). While the newly formed bond in **17a** is equatorial the second ring closure to **23a** results in both bonds being axial. Recently, Freeman et al. comprehensively analyzed the complex conformational interconversions of cycloheptane and some heterocycloheptanes.[43] Their CCSD/cc-pVDZ computations showed that the twist chair form of cycloheptane (observed in **18a**), lies 1.0 and 3.4 kcal mol^{-1} lower in energy than the chair (observed in **24a**) and boat (observed in **17a**) conformations, respectively. During the second ring closure, all low-lying conformers are converted to energetically less favorable conformations (Figure 6). For the fenestranes the (R*,**R***)-configuration is always favored, while the opposite is true for cyclooctatrienes. A summary of the conformational analyses for the systems of pathway II is available in Table 6.

Stereochemical Control in the 8π-Conrotatory Electrocyclization. a. Pathway I. The potential energy hypersurfaces (PES) of pathway I (Scheme 3) for the two (R*,**R***)- and (R*,**S***)-diastereomers are presented in Scheme 9. Cyclooctatriene **14** with (R*,**S***)-stereochemistry is the only experimentally observed product and is also the lowest-energy minimum on this part of the PES.[18] In contrast to pathway II (vide infra) involving cyclohexane ($n = 1$, Scheme 3), the kinetic product **14′** has not been observed experimentally.

b. Pathway II. The energy differences of the first transition structures control the (R*,**R***)- or (R*,**S***)-diastereoselectivities in the cascade reactions (Scheme 10). The six-membered ring TS toward the (R*,**R***)-stereoisomer is 0.9 kcal mol^{-1} lower in energy than toward (R*,**S***); this preference is reversed (3.1 kcal mol^{-1}) for the seven-membered ring. As a result, fenestrane **21a** is the kinetic product; the analogue fenestrane **23a** was not observed. On the pathway for **X** = 7 the cyclooctatriene **18a** is the kinetically as well as the thermodynamically favored product, in line with experiment. For both **X** = 6 and 7 the (R*,**S***)-configured cyclooctatrienes are the lowest-lying minima on this part of the PES. As discussed, the cycloalkane moieties of these structures show the most stable conformations and

Scheme 10. Potential Energy Hypersurfaces for the Two Possible Stereochemical Outcomes for **X** = 6 and 7[a]

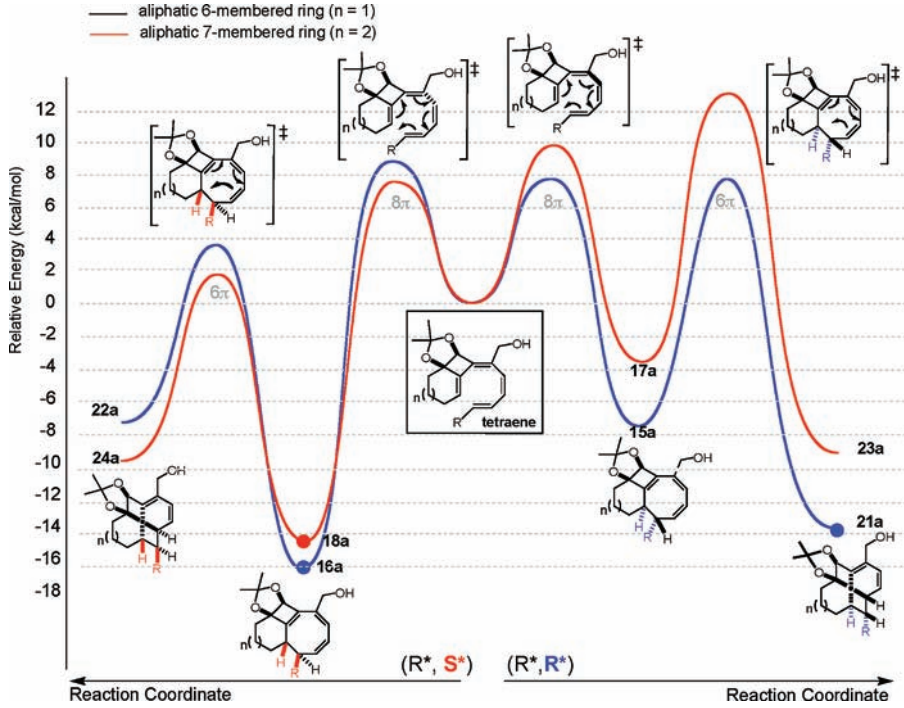

[a] The right part of the surface is responsible for the (R*,**R***) and the left part for the (R*,**S***) stereoisomers. The experimentally observed structures are determined by cycles.

Scheme 11. Surface Energy Potentials of the (R*,**R***)- (for **X** = 4−6) and (R*,**S***)-[4.**X**.4.6]Fenestradienes for **X** = 7 and 8

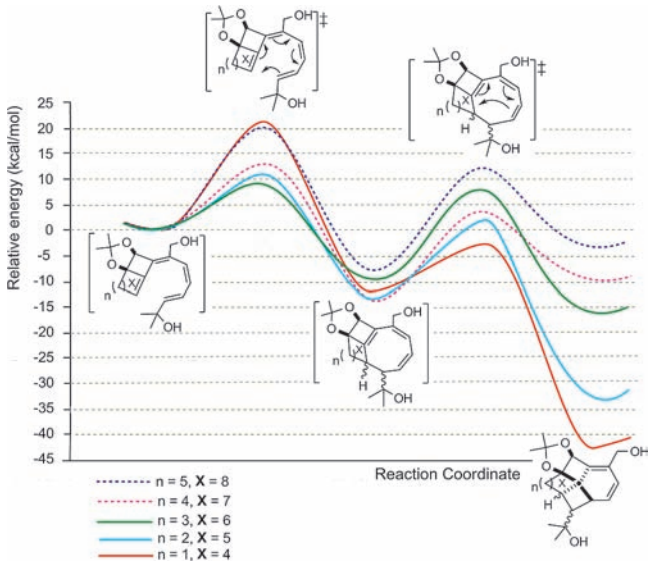

the newly formed bonds are in *equatorial* positions (Figure 6). The stabilities of (R*,**S***)-cyclooctatrienes relative to their valence isomers (R*,**S***)-fenestradienes are related to the high strain energies in fenestradienes (Table 6). The *trans* configuration of C^1-C^8 and C^2-C^7 in (R*,**S***)-fenestradienes are unfavorable; this is also evident from the C^2-C^7 bond lengthening (up to 1.59 Å, Table 6). As a consequence, **22a** and **24a** are 9.3 and 5.6 kcal mol^{-1}, respectively, less stable than the corresponding cyclooctatrienes. This agrees well with the experimentally found divergence in reactivity of the (R*,**S***)-cyclooctatrienes toward (R*,**S***)-fenestradienes.

c. Conversion of the Kinetic Product 21a to the Thermodynamic Stereoisomer 16a. The PES presented in Scheme 10 reveals that **16a** is the global minimum on this part of the PES, which, however, was not observed at the first. This stationary point is 9.3 and 1.7 kcal mol^{-1} more stable than **22a** (not observed) and **21a** (observed), respectively. Excitingly, the isolated fenestradiene **21a** after stirring in benzene at 110 °C under microwave irradiation for 30 min, converted completely into the valence isomer **16a** without degradation (IIc in Schemes 3 and 5).

Synthesis of [4.X.4.6]Fenestradienes versus Cyclooctatrienes. Correlations between the structural aspects and the stabilities derived from Table 6 and Scheme 10 provide insights into the synthesis of the [4.**X**.4.6]fenestradienes. The stability of the studied fenestradienes is not only a function of the bond angles $C(C)_4$, but is more influenced by the relative configurations at the rings (Figure 3 and Table 6). The results lead to the prediction that fenestradienes including small aliphatic rings with (R*,**R***) configuration may be stable enough kinetically or even thermodynamically to be isolated (Scheme 11). To investigate this prediction, the most strained four-membered aliphatic ring (**X** = 4) has been computed. The corresponding (R*,**S***)-fenestradiene dissociated at the quaternary carbon center during the optimization. The four-membered ring (R*,**R***)-fenestradiene is considerably more stable than the other two valence isomer (R*,**R***)- (−33 kcal mol^{-1}) and (R*,**S***)-cyclooctatrienes (−16 kcal mol^{-1}). Therefore, (R*,**R***)-fenestradiene for **X** = 4 would be the thermodynamic product of such a cascade reaction and is predicted to be isolable.

Conclusions

In the current work we present a full account of an efficient cascade reaction for the synthesis of unique and rarely discussed multicyclic cyclooctatrienes (c**X**) and fenestradienes (f**X**). This remarkable reaction was analyzed with the help of DFT computations.

The reaction cascade involves three consecutive transformations starting from dioxolane trienynes (**4** and **5**). A selective mild hydrogenation of the conjugated alkyne function starts the reaction. In this step P-2 Nickel catalyst (1 equiv.) prepared from $Ni(OAc)_2 \cdot 4\ H_2O$ and $NaBH_4$ yields the largest amount of product and quantitative conversion. The reaction proceeds toward c**X** through an 8π-conrotatory ring closure. The *s-cis* configurations of the terminal substituents through the conrotatory mode led to *trans* connections between C^1 and C^8 in all cases. In the third step, formations of the C^2-C^7 bonds in 6π-disrotatory electrocyclizations convert the triene cyclic moieties of c**X** to bicyclo[4.2.0]octadienes giving the valence isomers f**X**.

The hydrogenation of starting compound **4** (**X** = 6) at room temperature led to fenestradienes **21**, while at higher temperatures it gave stable cyclooctatrienes **16** with *opposite* torquoselectivity for the newly formed single C^1-C^8 bonds. For the starting compound **5** (**X** = 7) at any reaction temperature only cyclooctatrienes **18** with the same stereochemistry as their analogues **16** were observed.

Computations show that in the 8π-conrotatory ring closure toward c**X** the *M*- and *P*-helical orientations are possible for the Möbius aromatic tetraene chains of the transition structures. Orientations of the tetraene chains on the same and on opposite sides of the dioxolane moieties cause *M*- and *P*-helices, respectively. The *M*-helical Möbius aromatic transition structure leads to right handed-torquoselectivity (R*,**R***) while the *P*-helical topology gives the corresponding (R*,**S***)-diastereomers through a left-handed rotation of the terminal substituents.

The C^2-C^7 bonds that form in the next reaction step after the C^1-C^8 connections have a fixed orientation relative to the **X**-membered ring moieties. Structural analyses reveal that in the formation of a fenestradiene the C^1-C^8 bond requires *the same cis* orientation relative to C^2-C^7. This occurs through a *M*-helical transition structure corresponding to (R*,**R***)-configuration. The 6π-disrotatory electrocyclization step toward the fenestradienes avoids *P*-helical topology in the first transition structure and leads to (R*,**S***)-torquoselectivity and a *trans* configuration of these bonds.

While the (R*,**S***)-torquoselectivity causes considerable strain in the fenestradienes, it favors cyclooctatriene formation; in the corresponding c**X** the C^1-C^8 bonds are *equatorially* oriented and the cycloalkane moieties exhibit their most stable conformers. The new formed C^1-C^8 single bonds through the *M*- and *P*-helical topologies are directed in the *axial* (R*,**R***-configuration) and in the *equatorial* (R*,**S***-configuration) positions of the smaller cycloalkane rings, respectively. For t**X** involving seven- and eight-membered

(41) Ajami, D.; Oeckler, O.; Simon, A.; Herges, R. *Nature* **2003**, *426*, 819–821.
(42) Cope, A. C.; Haven, A. C.; Ramp, F. L.; Trumbull, E. R. *J. Am. Chem. Soc.* **1952**, *74*, 4867–4871.
(43) (a) Freeman, F.; Hwang, J. H.; Junge, E. H.; Parmar, P. D.; Renz, Z.; Trinh, J. *Int. J. Quantum Chem.* **2008**, *108*, 339–350. (b) Gill, G.; Pawar, D. M.; Noe, E. *A J. Org. Chem.* **2005**, *70*, 10726–10731.

olefinic rings *M*-helical transition structures as well as *P*-helices lead to *equatorial* C^1-C^8 connections. The higher flexibility of the larger neighboring cycloalkanes makes this possible. However, the formation of *equatorial* C^1-C^8 bonds through the (R*,**R***)-torquoselectivity leads to unfavorable conformations for the cycloalkane moieties. As a result, the *M*-helical transition structure and in the following a (R*,**R***)-fenestradiene valence isomer can not be observed for t**X** involving large **X**-membered ring moieties (**X** = 7 and 8). Only observed (R*,**S***)-cyclooctatrienes **18** for **X** = 7 in different reaction conditions confirm the computational results. The computed potential energy surfaces show that for c**X** involving smaller aliphatic ring moieties (**X** = 4−6) the (R*,**R***)-fenestradienes are indeed the kinetic products that can be isolated. For **X** = 7 and 8 the reaction cascades lead to (R*,**S***)-cyclooctatrienes kinetically and thermodynamically.

Acknowledgment. We are grateful to the CNRS for financial support. We thank the MNERT (C.H.) and the DAAD and Gottlieb Daimler- and Karl-Benz-Foundation (S.A.) for fellowships, and Professor Junes Ipaktschi for helpful discussions.

Supporting Information Available: Full experimental and computational details are available. Complete ref 35. This material is available free of charge via the Internet at http://pubs.acs.org.

JA903914R